AIAA SciTech Forum
4-8 January 2016, San Diego, California, USA
AIAA Atmospheric Flight Mechanics Conference

10.2514/6.2016-0017



# Minimum-Time Transition of FWMAVs from Hovering to Forward Flight

Ahmed Hussein* Haithem E. Taha† Muahmmed R. Hajj‡

**Unlike conventional airplanes, flapping-wing micro-air-vehicles (FWMAVs) move their wings continuously with respect to the body. These new degrees of freedom for the wings (wing kinematics) provide more room for optimal design of these miniature vehicles that are prone to stringent weight and power constraints. However, very few attempts have aimed to provide maneuverability-optimum wing kinematics. In general, the shapes of the kinematic functions are assumed from the outset and their level of control authority is assessed at a later stage. In this work, we formulate a minimum-time optimal control problem to steer the FWMAV dynamical system from hovering configuration to forward flight with a prescribed forward speed. Assuming horizontal stroke plane and a piece-wise constant variation for the wing pitching angle, only the waveform of one degree-of-freedom for the wing is optimized (back and forth flapping). Since the flapping angle is periodic, we represent it via a truncated Fourier series. The number of Fourier terms is discussed. The optimal control problem is formulated such that the cost functional is the final time, the slowly time-varying Fourier coefficients of the flapping angle are the inputs to be optimized along with the angles of attack (i.e., design variables), and the goal is to steer the averaged dynamics from the hovering configuration (origin) to a prescribed forward speed.**



## Nomenclature

| | |
|---|---|
| $c$ | Chord length |
| $\bar{c}$ | Mean chord length |
| $g$ | Gravitational acceleration |
| $m$ | Body mass |
| $M$ | Aerodynamic moment about $y_b$ axis |
| $I_y$ | Body moment of inertia about the yb axis |
| $r$ | Distance along the wing span |
| $\bar{r}$ | Radius of section having mean chord length |
| $R$ | Wing radius (Length) |
| $S$ | Area of one wing |
| $t$ | Time variable |
| $T, f$ | Flapping period and frequency |
| $X$ | Aerodynamic force along $x_b$ axis |
| $Z$ | Aerodynamic force along $z_b$ axis |
| $\hat{x_0}$ | Normalized position of the pitch axis |
| $\Delta\hat{x}$ | Normalized chordwise distance between the center of pressure and the hinge location |
| $\alpha$ | Angle of attack |
| $\eta$ | Pitching angle of the wing |
| $\varphi$ | Back and forth flapping angle |
| $\Phi$ | Amplitude of the flapping motion |
| $\theta$ | Pitching angle of the body |
| $\rho$ | Air density |

## I. Introduction

Unlike conventional airplanes, flapping-wing micro-air-vehicles (FWMAVs) move their wings continuously with respect to the body. These new degrees of freedom for the wings trigger a whole new area of research to answer

*PhD student,Department of Biomedical and Engineering Mechanics, Virginia Tech., Blacksburg
†Assistant Professor, Department of Mechanical and Aerospace Development, University of California, Irvine
‡Professor, Department of Biomedical and Engineering Mechanics, Virginia Tech., Blacksburg

the following questions: What should be the wing motion for optimum aerodynamic performance?, What should the wing kinematics look like for maximum maneuverability from an equilibrium position?, and several other questions. The optimization objective for flapping-wing micro-air-vehicles is necessary because of the stringent weight, size, and power constraints imposed on the design of these miniature vehicles.

While we find many interesting research articles aiming for aerodynamic-optimum wing kinematics, very few trials have aimed to provide maneuverability-optimum wing kinematics. Berman and Wang [1], Kurdi et al. [2], and Taha et al. [3] formulated optimization problems to determine the optimal time variations of the Euler angles, describing flapping kinematics, for hovering with minimum aerodynamic power. Stanford and Beran [4] and Ghommem et al. [5] solved similar problems for optimum aerodynamic performance in forward flight. On the other hand, the open literature, indeed, lacks constructive techniques to determine maneuverability- or control-optimum kinematics. The common approach is to assume the shape of the kinematic functions from the outset and adapt such a shape to ensure controllability for the FWMAV, see Schenato et al. [6], Doman et al. [7], and Oppenheimer et al. [8]. That is, the kinematic functions are not derived. For a more detailed information about kinematic optimization of FWMAVs, the reader is referred to the thorough review article by Taha, Hajj, and Nayfeh [9].

The first trial to provide a constructive approach for maneuverability-optimum kinematics was proposed by Taha et al. [10]. They used calculus of variations and optimal control to determine the optimum waveform for the back and forth flapping angle in a horizontal stroke plane and constant angle of attack that results in the maximum cycle-averaged forward acceleration from a hovering position. Since Taha et al. considered the initial acceleration from a hovering equilibrium, they neglected the body dynamics and, as such, the problem is simplified to a one-degree-of-freedom kinematic optimization problem. Therefore, they could even solve it using calculus of variations techniques.

In this work, we formulate a minimum-time optimal control problem to determine the evolution of the optimum wing kinematics that steers the FWMAV dynamical system from a hovering configuration to a forward flight configuration with a prescribed forward speed. Since flapping flight dynamics constitutes a nonlinear, time-periodic system, equilibrium configurations (e.g., hovering and forward flight) are represented by periodic orbits. As such, the optimal steering problem between different equilibrium configurations becomes intricate. In fact, ensuring equilibrium is difficult. Therefore, we rely on the large separation between the FWMAV system's two time scales (fast time scale associated with flapping and slow time scale associated with body motion dynamics). to use the averaging theorem to convert the time-periodic flapping flight dynamics into a time-invariant system. As such, the periodic orbits representing equilibrium of the original time-periodic system are reduced to fixed points. Clearly, steering between fixed points is quite easier than steering between periodic orbits.

Following most insects in nature [11, 12], a horizontal stroke plane is assumed here, with a stroke plane angle $\varphi$. Moreover, the wing pitching angle $\eta$ is assumed to be passively controlled with the back and forth flapping angle $\varphi$ in such a way to maintain a constant angle of attack throughout the entire stroke. In fact, these kinematics have been extensively used in the literature of hovering FWMAVs [6, 7, 8, 13, 3], as they comply with minimum actuation requirements in FWMAVs, stressed as the main reason for the successful flapping flight of the Harvard Robofly [14]. Figure 1 shows a schematic diagram for a FWMAV performing a horizontal stroke plane.

The main technical challenge facing optimal control formulation for FWMAVs kinematic optimization is the periodicity constraint. We go about this challenge by exploiting the periodicity nature of the flapping angle $\varphi$ to write its waveform over one cycle in a truncated Fourier series expansion. The required number of Fourier terms is discussed. Over a flapping cycle (i.e., fast time scale), the Fourier coefficients of the flapping angle waveform are constants. However, since the waveform may vary from one cycle to another (e.g., symmetric waveform is expected at hovering while asymmetric waveform is expected during forward flight), the Fourier coefficients will be slowly time-varying. As such, we formulate an optimal control problem such that the final time is the cost functional (i.e., minimum-time problem), the controls to be optimized are the slowly-varying Fourier coefficients of the $\varphi$-waveform, and the controls have to steer the FWMAV averaged dynamics (slowly varying dynamics) from a hovering fixed point to a forward flight fixed point.

# II. Flight Dynamic Model

We use a flight dynamic model that was developed in a previous work [15, 16]. This model neglects flexibility wing-inertial effects. As for aerodynamics, it uses a quasi-steady formulation that accounts for the dominant leading

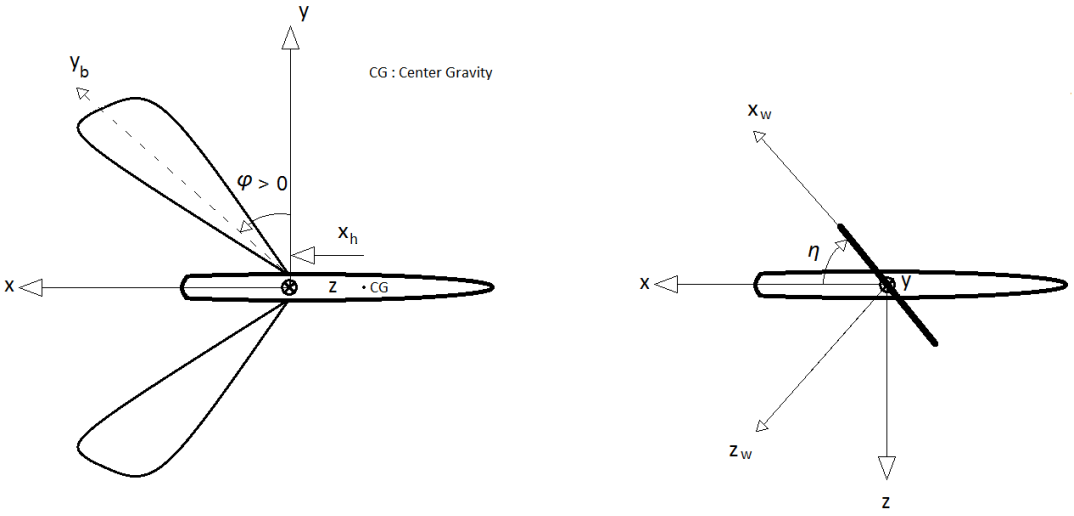


Figure 1: Schematic diagram showing the back-and-forth flapping angle $\varphi$ and the pitching angle of the wing $\eta$.

edge vortex contribution as well as rotational effects. The model is written as

$$\begin{pmatrix} \dot{u} \\ \dot{w} \\ \dot{q} \\ \dot{\theta} \end{pmatrix} = \begin{pmatrix} -qw - g\sin\theta \\ qu + g\cos\theta \\ 0 \\ q \end{pmatrix} + \begin{pmatrix} \frac{1}{m}X_o(t) \\ \frac{1}{m}Z_o(t) \\ \frac{1}{m}M_o(t) \\ 0 \end{pmatrix} + \begin{pmatrix} X_u(t) & X_w(t) & X_q(t) & 0 \\ Z_u(t) & Z_w(t) & Z_q(t) & 0 \\ M_u(t) & M_w(t) & M_q(t) & 0 \\ 0 & 0 & 0 & 0 \end{pmatrix} \begin{pmatrix} u \\ w \\ q \\ \theta \end{pmatrix} \tag{1}$$

where $u$ is the forward velocity component along the body $x$ axis, $w$ is the normal velocity component along the body $z$ axis, and $\theta$ and $q$ are pitching angle and angular velocity of the body, respectively. In Eq. (1), $X_0$, $Z_0$ and $M_0$ are the aerodynamic forces due to flapping and the drag of the body. They can be written as :

$$\begin{aligned} X_0(t) &= -2K_{21}\dot{\varphi}(t)|\dot{\varphi}(t)|\cos\varphi(t)\sin^2\eta - \frac{1}{2}\bar{\rho_b}S_bC_{D_b}Vu \\ Z_0(t) &= -K_{21}\dot{\varphi}(t)|\dot{\varphi}(t)|\sin 2\eta - \frac{1}{2}\bar{\rho_b}S_bC_{D_b}Vw \\ M_0(t) &= 2\dot{\varphi}(t)|\dot{\varphi}(t)|\sin\eta(K_{22}\Delta\hat{x}\cos\varphi(t) + K_{21}x_h\cos\eta + K_{31}\sin\varphi(t)\cos\eta \end{aligned}$$

where $K_{mn} = 1/2\rho AI_{mn},\ I_{mn} = 2\int_0^R r^m c^n(r)dr,\ S_b = \pi D_b L_b$ and $D_b/L_b = \left(4m_b/(\pi\bar{\rho_b}L_b^3)\right)^{0.5}$ .

The stability derivatives $\bar{X}_u$, $\bar{X}_w$, $\bar{X}_q$, $\bar{Z}_u$, $\bar{Z}_w$, $\bar{Z}_q$, $\bar{M}_u$, $\bar{M}_w$ and $\bar{M}_q$ represent the aerodynamic loads due to body

motion variables. They are given by

$$
\begin{aligned}
X_u(t) &= -4\frac{K_{11}}{m}|\dot{\varphi}(t)|\cos^2\varphi(t)\sin^2\eta \\
X_w(t) &= -\frac{K_{11}}{m}|\dot{\varphi}(t)|\cos\varphi(t)\sin 2\eta \\
X_q(t) &= \frac{K_{21}}{m}|\dot{\varphi}(t)|\sin\varphi(t)\cos\varphi(t)\sin 2\eta - x_h.X_w(t) \\
Z_u(t) &= 2X_w(t) \\
Z_w(t) &= -2\frac{K_{11}}{m}|\dot{\varphi}(t)|\cos^2\eta \\
Z_q(t) &= 2\frac{K_{21}}{m}|\dot{\varphi}(t)|\sin\varphi(t)\cos^2\eta - \frac{K_{rot_{12}}}{m}\dot{\varphi}(t)\cos\varphi(t) - x_h Z_w(t) \\
M_u(t) &= 4\frac{K_{12}\Delta\hat{x}}{I_y}|\dot{\varphi}(t)|\cos^2\varphi(t)\sin\eta + \frac{m}{I_y}(2X_q - x_h Z_u(t)) \\
M_w(t) &= 2\frac{K_{12}\Delta\hat{x}}{I_y}|\dot{\varphi}(t)|\cos\varphi(t)\cos\eta + 2\frac{K_{21}}{I_y}|\dot{\varphi}(t)|\sin\varphi(t)\cos^2\eta - \frac{m.x_h}{I_y}Z_w(t)
\end{aligned}
$$

$$
\begin{aligned}
M_q(t) = &-\frac{2\Delta x}{I_y}|\dot{\varphi}(t)|\cos\varphi(t)\cos\eta(K_{12}x_h + K_{22}\sin\varphi(t)) + \frac{1}{I_y}\dot{\varphi}(t)\cos\varphi(t)(K_{rot_{13}}\Delta\hat{x}\cos\varphi(t)\cos\eta + K_{rot_{22}}\sin\varphi(t)) \\
&- \frac{2}{I_y}|\dot{\varphi}(t)|\cos^2\eta\sin\varphi(t)(K_{21}x_h + K_{31}\sin\varphi(t)) - \frac{K_v\mu_1 f}{I_y}\cos^2\varphi(t) - \frac{mx_h}{I_y}Z_q(t)
\end{aligned}
$$

where $K_{rot_{mn}} = \pi\rho(1/2 - \Delta\hat{x})I_{mn}$ and $K_v = \pi/16\rho I_{04}$ .

The system (1) can be written in an abstract form as

$$\dot{\boldsymbol{\chi}} = \boldsymbol{f}(\boldsymbol{\chi}) + \boldsymbol{g}(\boldsymbol{\chi}, \varphi(t)) \tag{2}$$

where the state vector $\boldsymbol{\chi} = [u, w, q, \theta]^T$, $\boldsymbol{f}$ is the inertial and gravitational contributions, and $\boldsymbol{g}$ represents the time-periodic aerodynamic loads that are written affine in the state variables.

# III. The Averaging Approach

Equation (2) is a nonlinear time-periodic (NLTP) system whose stability analysis and control design is challenging. A very convenient way of transforming the NLTP system (1) into a representative time-invariant system is the averaging approach. This approach is mainly based on the assumption that, due to the very fast flapping frequency relative to the body dynamics, the body only feels the average values of the aerodynamic loads. It should be noted that the ratio of the flapping frequency to the body natural frequency for the slowest flapping insect (Hawkmoth) is about 30 [16]. For man made FWMAVs (e.g., Harvard Robofly), the ratio may even reach as high as 120. In fact, the averaging approach is mathematically justified (based on the stated assumption) in the following theorem.

## *A. Averaging Theorem*

For a nonlinear, time-periodic system in the form

$$\dot{\boldsymbol{\chi}} = \epsilon\boldsymbol{Y}(\chi, t, \epsilon) \tag{3}$$

where $\boldsymbol{Y}$ is $T$-periodic, define the averaged dynamics as [17]

$$\dot{\bar{\boldsymbol{\chi}}} = \epsilon\bar{\boldsymbol{Y}}(\bar{\boldsymbol{\chi}}) = \epsilon\frac{1}{T}\int_0^T \boldsymbol{Y}(\bar{\boldsymbol{\chi}}, t).dt \quad \text{where } \epsilon \ll 1 \tag{4}$$

If the averaged system (4) has a *hyperbolic* fixed point, then the original NLTP system (3) will have a hyperbolic periodic orbit of the same stability type [17, 18]. That is, the averaged dynamics is representative for the time-periodic system as well as $\epsilon$ is small enough.

### B. Averaged Dynamics

Recall the abstract form (2) of the used flight dynamic model, and to write it in the form (3) that is amenable to the averaging theorem, we introduce a new time variable $\tau = \omega t$, where $\omega$ is the flapping frequency. The system (2) is then written as

$$\frac{d\boldsymbol{\chi}}{d\tau} = \frac{1}{\omega}(\boldsymbol{f}(\boldsymbol{\chi}) + \boldsymbol{g}(\boldsymbol{x}, \varphi(\tau)) \tag{5}$$

which is in the form (3) with $\epsilon = \frac{1}{\omega}$. That is, if flapping is performed with a high enough frequency, $\epsilon$ would be small enough to apply the averaging theorem.

Averaging the system (5) and transforming it back to the original time variable, we obtain

$$\dot{\bar{\boldsymbol{\chi}}} = \boldsymbol{f}(\bar{\boldsymbol{\chi}}) + \bar{\boldsymbol{g}}(\bar{\boldsymbol{\chi}}) \tag{6}$$

where $\bar{\boldsymbol{g}}(\boldsymbol{\chi}) = \frac{1}{T}\int_0^T \boldsymbol{g}(\boldsymbol{\chi}, \varphi(t))dt$ represents the cycle-averaged aerodynamic loads. As such, the averaged dynamics of the system (1) is written as

$$\begin{pmatrix} \dot{\bar{u}}(t) \\ \dot{\bar{w}}(t) \\ \dot{\bar{q}}(t) \\ \dot{\bar{\theta}}(t) \end{pmatrix} = \begin{pmatrix} -\bar{q}(t)\bar{w}(t) - g\sin\bar{\theta}(t) \\ \bar{q}\bar{u}(t) + g\cos\bar{\theta}(t) \\ 0 \\ \bar{q}(t) \end{pmatrix} + \begin{pmatrix} \frac{1}{m}\bar{X}_o(t) \\ \frac{1}{m}\bar{Y}_o(t) \\ \frac{1}{m}\bar{Z}_o(t) \\ 0 \end{pmatrix} + \begin{pmatrix} \bar{X}_u(t) & \bar{X}_w(t) & \bar{X}_q(t) & 0 \\ \bar{Z}_u(t) & \bar{Z}_w(t) & \bar{Z}_q(t) & 0 \\ \bar{M}_u(t) & \bar{M}_w(t) & \bar{M}_q(t) & 0 \\ 0 & 0 & 0 & 0 \end{pmatrix} \begin{pmatrix} \bar{u}(t) \\ \bar{w}(t) \\ \bar{q}(t) \\ \bar{\theta}(t) \end{pmatrix} \tag{7}$$

where over bar denotes an averaged quantity. It should be noted that although the variables in the averaged system (7) are averaged over the flapping cycle (fast time-scale), they are still slowly time-varying as the FWMAV maneuvers (i.e., moves from one equilibrium configuration to another).

## IV. Optimal Control Formulation

Since the back-and-forth flapping angle $\varphi$ is periodic, it can be written over one period in a truncated Fourier series expansion as

$$\varphi(\tau) = a_0 + \sum_{n=1}^{N}(a_n\cos(\frac{2\pi n}{T}\tau + b_n\sin(\frac{2\pi n}{T}\tau)) \tag{8}$$

where $\tau$ is the fast time scale. If we substitute for $\varphi$ from Eq. (8) into the aerodynamic loads (e.g., $X_0$-$M_0$ and stability derivatives) and then integrate the outcomes to obtain the corresponding cycle-averaged quantities (e.g., $\bar{X}_0$-$\bar{M}_0$ and cycle-averaged stability derivatives), the averaged dynamics (7) will be written as

$$\dot{\bar{\boldsymbol{\chi}}}(t) = \boldsymbol{F}(\bar{\boldsymbol{\chi}}(t), \boldsymbol{U}(t)) \tag{9}$$

where $\boldsymbol{U} = \begin{bmatrix} a_0 & \boldsymbol{a} & \boldsymbol{b} & \alpha_u & \alpha_d \end{bmatrix}$ contains the Fourier coefficients of the flapping angle $\varphi$, which are slowly time-varying for a varying waveform during a maneuver execution and angles of attack during the upstroke and down stroke respectively. That is, the Fourier coefficients $\underline{a} = (a_1, a_2, ..., a_N)$ , $\underline{b} = (b_1, b_2, ..., b_N)$ and $\alpha_u, \alpha_d$ are seen as inputs to the averaged dynamics.

Then, the optimal control problem is to find a piecewise continuous control $\boldsymbol{U}(.) : [0, t_f^*] \rightarrow [-1, 1]^{2N+1} \subset \mathbb{R}^{2N+1}$ that steers the system (9) from the origin to the point $[V_f, 0, 0, 0]^T$, where $V_f$ is the specified desired forward speed and minimizes the functional $J(\boldsymbol{U}(.)) = \int_0^{t_f^*} 1dt$ (i.e., steering in minimum time). Clearly, the final time is unknown and should be come with the solution of the optimal control problem. The optimal control problem can be defined as follows :

$$min\ J(\boldsymbol{U}(.)) = \int_0^{t_f^*} 1dt = t_f^* \tag{10}$$

satisfies the differential equation of

$$\dot{\bar{\boldsymbol{\chi}}}(t) = \boldsymbol{F}(\bar{\boldsymbol{\chi}}(t), \boldsymbol{U}(t)) \tag{11}$$

Subject to end constraints

$$\begin{aligned} \dot{\bar{\boldsymbol{\chi}}}(t_f^*) = 0,\ V_x(t_f^*) = V_f \\ V_z(t_f^*) = 0,\ q(t_f^*) = 0 \end{aligned} \tag{12}$$

and path constraints

$$\begin{aligned} \boldsymbol{U}_L \leq \boldsymbol{U}(t) \leq \boldsymbol{U}_U \\ \varphi_L \leq (\varphi_{max}(t), \varphi_{min}(t)) \leq \varphi_U \\ V_{z_L} \leq V_z \leq V_{z_U} \\ \begin{pmatrix} u_L \\ w_L \\ q_L \\ \theta_L \end{pmatrix} \leq \begin{pmatrix} u(t) \\ w(t) \\ q(t) \\ \theta(t) \end{pmatrix} \leq \begin{pmatrix} u_U \\ w_U \\ q_W \\ \theta_U \end{pmatrix} \end{aligned} \tag{13}$$

The end constraint $\dot{\tilde{\boldsymbol{\chi}}}(t_f^*) = 0$ is introduced to ensure equilibrium at the final conditions. The path constraint imposed on the body angle $\theta$ and the minimum, maximum flapping angle $\varphi_{max}(t), \varphi_{min}(t))$ is chosen such that it doesn't exceed the physical ability of the MAV.

In order to overcome the problem of choosing higher numbers of Fourier coeffeicents we use another function for the flapping angle defined by Bhatia et al.[20]. This function was first introduced by Berman and Wang [1] for the symmetric flapping during hovering and was later modifed by Doman et al. [21] to account for asymmetric flapping and continuity beteween cycles. We will adopt here the function of Bhatia et al.[20] which differs from Doman et al.[21] in how they define the continuity criteria. The flapping angle without the continuity criteria of Bhatia et al.[21] is adopted at this stage as it will be showed later that no feasible solution is obtained when using this criteria. The flapping angle can be defined as follows:

$$\varphi(\tau) = \begin{cases} \phi_m \frac{sin^{-1}\{K_\phi sin[(\omega-\delta)t+\pi 2]\}}{sin^{-1}K_\phi} + \phi_0, & 0 \leqq t \leqq \frac{\pi}{\omega-\delta} \\ \phi_m \frac{sin^{-1}\{K_\phi sin[\tilde{\omega}t+\tilde{\zeta}+\pi 2]\}}{sin^{-1}K_\phi} + \phi_0, & \frac{\pi}{\omega-\delta} \leqq t \leqq \frac{2\pi}{\omega} \end{cases} \tag{14}$$

where $\tilde{\omega} = \frac{\omega(\omega-\delta)}{\omega-2\delta}$ and $\tilde{\zeta} = \frac{-2\pi\delta}{\omega-2\delta}$.

The optimal control problem will be the same as defined in Eq.10 satisfying Eq.11 subjected to Eqs.[12,13] but with a new vector of input $\boldsymbol{U} = \begin{bmatrix} \delta & \phi_0 & \phi_m & K_\phi & \alpha_u & \alpha_d \end{bmatrix}$. Equation 14 allows more freedom in the resulting shape of the flapping angle using only four inputs while preserving the wave monotonicity. The input that control the shape of waveform is $K_\phi$. The value of $K_\phi = 1$ represents a triangular wave while the case of $K_\phi \ll 1$ represents a sinusoidal wave.

# V. Solution of the Optimal Control Problem

## A. *Trim Solution*

Before starting to solve the optimal control problem, we should make sure that the final forward speed requirement is achievable. To do so, a simple optimization problem whose objective function is the minimum square error of the inertial velocities and the final equilibrium conditions subjected to the path equations of Eq12 is to be solved. It can be written as follows :

$$\min_{\boldsymbol{x}} \sum [\left(V_x(t_f^*) - V_f\right)^2 + V_z(t_f^*)^2 + \dot{\tilde{\boldsymbol{\chi}}}(t_f^*)^2] \tag{15}$$

subjected to the path constraints defined in Eq.12. Where $\boldsymbol{x} = [a_0 \ \boldsymbol{a} \ \boldsymbol{b} \ \alpha_u \ \alpha_d \ u \ w \ \theta]$, is the vector of the design variable

The Hawkmoth parameters used in this study, and the values used for the lower and upper bounds of the inputs, states and the end conditions are tabluated in Table1 and Table3 respectively. The values of the final value column which are left blank are part of the solution. The results of the optimization problem are tabulated in Table[2]. The minimum values of the error obtained form this optimization for forward speed $V_f = 2m/s$ using three and five Fourier coeffeicents were $8.6e^{-14}$ and $4.02e^{-13}$ respectively, which means that the forward speed requirement is feasible. This result agrees well with the expiremental observations done by Willmott and Ellington [22] which indicated that the normal range of the hawkmoth flight speed is $[0-5]m/s$. Now we proceed further to solve the optimal control problem as it is physically well posed.

## B. *Optimal Control Solution*

The optimal control problem defined by Eqs 10, 11, 12 is then solved using ICLOCS software. Figures [2] depicts three solutions of the time histories of the body states obtained for three Fourier coeffeicents $a_0, a_1, b_1, \alpha_u, \alpha_d$ , five

Table 1: Hawkmoth parameters

| Constant | Value | Constant | Value |
|---|---|---|---|
| $\bar{r_1}$ | 0.44 | $m_b$ | $1.648(mg)$ |
| $\bar{r_2}$ | 0.508 | $I_y$ | $2.08(g/cm^2)$ |
| $a_0$ | $2\pi$ | $f$ | $26.3(Hz)$ |
| $S_w$ | $947.8(cm^2)$ | $\Delta\hat{x}$ | 0.05 |
| $R$ | $51.9(mm)$ | $\Phi$ | $60.5^o$ |
| $\bar{c}$ | $18.3(mm)$ | $C_{D_b}$ | 0.7 |
| $D_b/L_b$ | 0.81 | $\bar{\rho_b}$ | $1100(Kg/m^3)$ |

Table 2: Optimization results

| Variable | $a_0(deg)$ | $\boldsymbol{a}(deg)$ | $\boldsymbol{b}(deg)$ | $\alpha_u(deg)$ | $\alpha_d(deg)$ | $u(m/s)$ | $w(m/s)$ | $\theta(deg)$ |
|---|---|---|---|---|---|---|---|---|
| Hovering | 60.5 | 0 | 0 | 0 | 0 | 0 | 0 | 0 |
| Forward(3FC) | -0.02 | -0.19 | -0.18 | 44.9 | 48.9 | 1.81 | 0.86 | 25.5 |
| Forward(5FC) | 3.94 | {1.7,1.84} | {-4.51,5.5} | 45.8 | 45.8 | 1.9262 | 0.54 | 15.6 |

Fourier coeffeicents $a_0, a_1, b_1, a_2, b_2, \alpha_u, \alpha_d$ and four coeffeicents $\phi_m, \phi_o, \delta, K_\phi, \alpha_u, \alpha_d$ for a initial guess for the final time of $T_{f_g} = 25T$ . It can be noticed from the Figures [2,a,b,c,d] that the equilibrium constraint is statisfied at the begining of the last two cycles. Figure [2-a] indicates that the body attitude is always negative for the three different cases of inputs. The case of Bhatia et al. is the most lower body pitch at the final time. These negative valuse of body pitch $\theta$ agrees with the concept of helicopter that the vehicle have to pitch down in order to move forward.

The time histories of the angles of attack $\alpha_u, \alpha_d$, mean flapping angle $\phi_m$, inertial velocities $V_x, V_z$, trajectory $H, X$ is shown in Figures[4a,b,c,d] respcetively. The change of the angles of attack during the different cycles indicates that a forward thrust is generated as the upstroke angle of attack is always greater than the down stroke angle of attack for the case of Fourier inputs. For the case of Bhatia et al., the upstroke angle of attack is almostly greater than the down stroke angle of attack except at the last two cylces. This may be interpreted as when the hawkmoth reaches an equilibrium state there is no need to generate more forward thrust to accelerate.

Despite the discrepancies between the time histories of the inputs,states and flight paths and the number of inputs, they all end up with the same final time. This means that there is no unique solution satisfies the end conditions at the same minimal final time. Figures [3,a,b,c,d,e,f] depicts the time history of the flapping angle for the different type of inputs. The case of the three and five Fourier coeffeicents have three or four discontinuites between cylcles in the range of $[0^0 - 10^0]$. The case of Bhatia et al. has much greater discontinuity particulary after the fourth cylce and have some constant flapping angle in a three concecutive cycles. These results show that the continuity of the flapping angle is an inevitable constraint. It shoud be noted that no feasible solution that satisfies all the boundary constraints and equlibrium was obtained when appplying the continuity constraint. In addition to the discontinuity of the flapping angle, the monotonicity of the flapping waveform should be conserved during the evoultion of the cycles. For instance, the monotonicity of the flapping angle for the five Fourier coeffeicents is sustained only for the first four cycles. This issue motivates the need for using the flapping waveform definedin Eq.14 [1, 21, 20].

# Conclusion

In this work, a simplified flight dynamic model for a flapping-wing micro-air-vehicle performing a horizontal stroke plane is considered. An optimal control problem is formulated to determine the evolution of the optimum waveform for the flapping angle in the horizontal plane that results in minimum-time transition from hovering to forward flight.The averaging theorem is used to transform the nonlinear, time-periodic flapping flight dynamics into a time-invariant system. The waveform of the flapping angle is represented in a truncated fourier series. The appropriate number of Fourier terms is discussed. The slowly-varying Fourier coefficients during maneuvers are seen as inputs to the averaged dynamics. As such, the problem is formulated to determine the optimum evolution of the Fourier coefficients that steers the averaged dynamics from a hovering equilibrium to a forward flight equilibrium. The time history of the flapping angle results from using the Fourier coefficents as inputs and Bhatia et al. function indicates that there is no unique solution to satisfy the objective. Also the use of the Bhati et al. waveform shows the power of

Table 3: Input and State Bounds

| Variable | Lower Bound | Upper Bound | Final Value |
|---|---|---|---|
| $t_0$ | 0 | 0 | 0 |
| $t_f$ | $20T$ | $1000T$ | – |
| $u(m/s)$ | 0 | 5 | – |
| $w(m/s)$ | -5 | 5 | – |
| $q(rad/s)$ | -100 | 100 | 0 |
| $\theta(rad)$ | $-\pi/2$ | $\pi/2$ | – |
| $\phi_{min,max}(rad)$ | $-\pi/2$ | $\pi/2$ | – |
| $[a_0,\ \boldsymbol{a},\ \boldsymbol{b}]\ (rad)$ | $-\pi/2$ | $\pi/2$ | – |
| $[\alpha_u,\ \alpha_d]\ (rad)$ | $-\pi/2$ | $\pi/2$ | – |
| $V_z(m/s)$ | 0 | 0 | 0 |
| $V_x(m/s)$ | 2 | 2 | 2 |

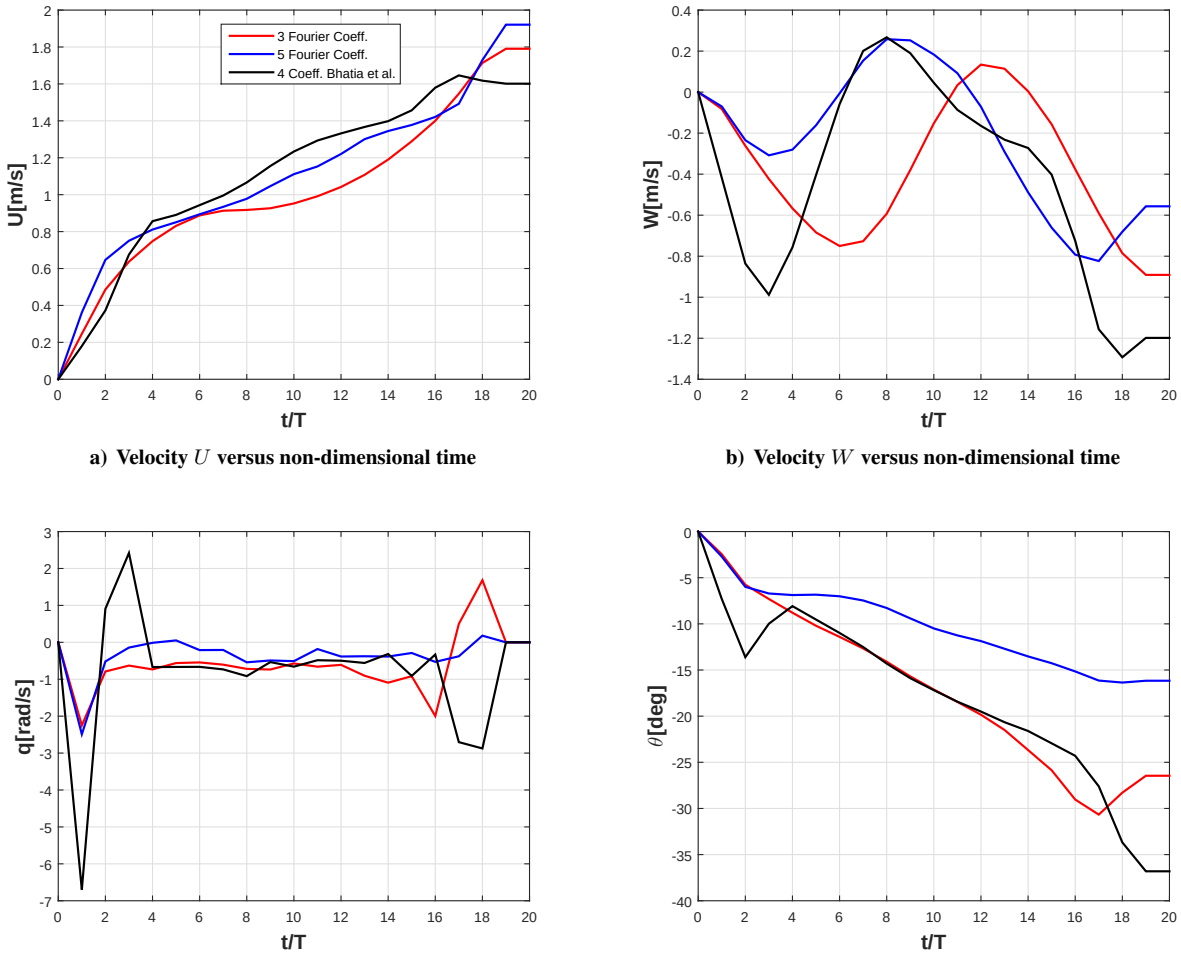


**a) Velocity $U$ versus non-dimensional time**

**b) Velocity $W$ versus non-dimensional time**

**c) Angular velocity $q$ versus non-dimensional time**

**d) Orientation $\theta$ versus non-dimensional time**

Figure 2: Time history of body variables for different initial guess of the final time using five inputs

mainting the wave monotoncity while capturing any kind of waveforms. Finally, it has to be pointed out the continuity constraint of the flapping angle yields a nonfeasible solution when it was imposed on the problem.

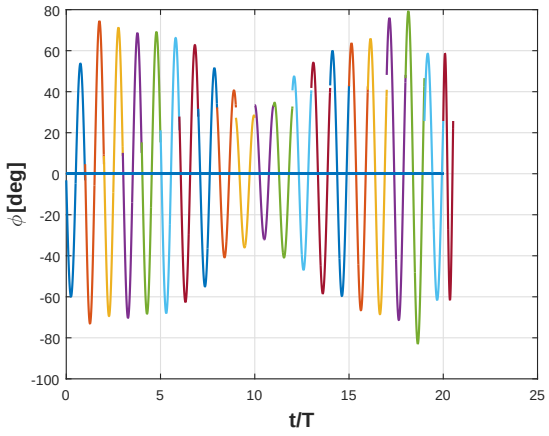


**a) Time history of flapping angle $\phi$ for 3 Fourier coeffeicents**

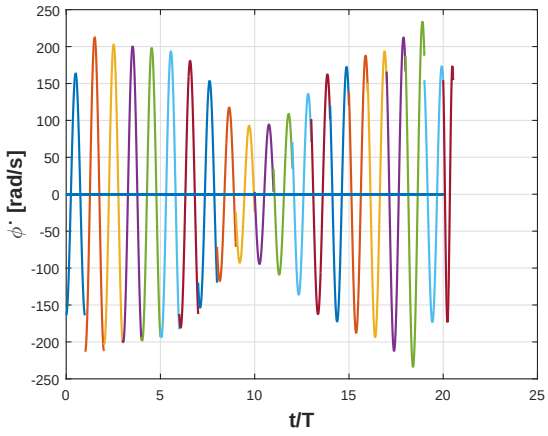


**b) Time history of rate of change of flapping angle $\dot{\phi}$ for 3 Fourier coeffeicents**

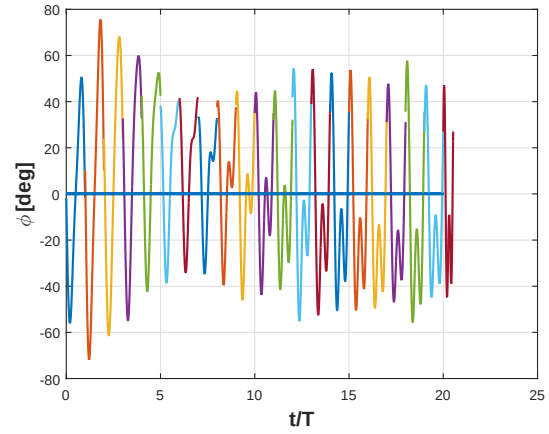


**c) Time history of flapping angle $\phi$ for 5 Fourier coeffeicents**

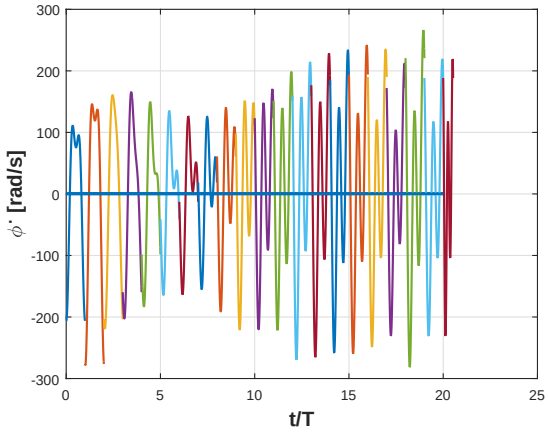


**d) Time history of rate of change of flapping angle $\dot{\phi}$ for 5 Fourier coeffeicents**

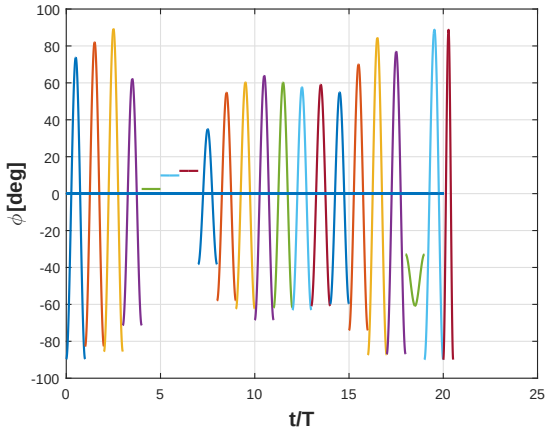


**e) Time history of flapping angle $\phi$ for 4 coeffeicents, Bhatia et al.**

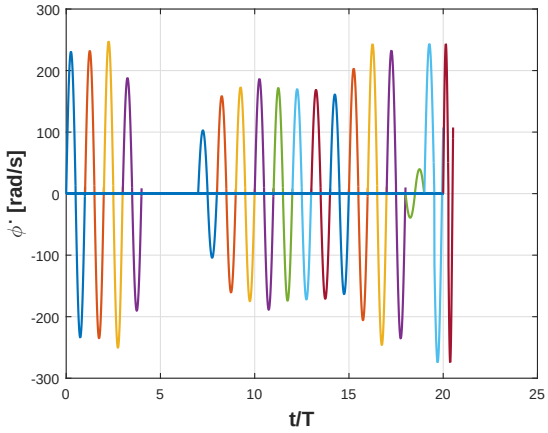


**f) Time history of rate of change of flapping angle $\dot{\phi}$ for 4 coeffeicents, Bhatia et al.**

Figure 3

# Acknowledgment

The authors acknowledge the support of the NSF Grant CMMI-1435484. The first author acknowledges the help of Mr. Guillaume Fraysse at the French Airforce Academy when he was visiting UCI.

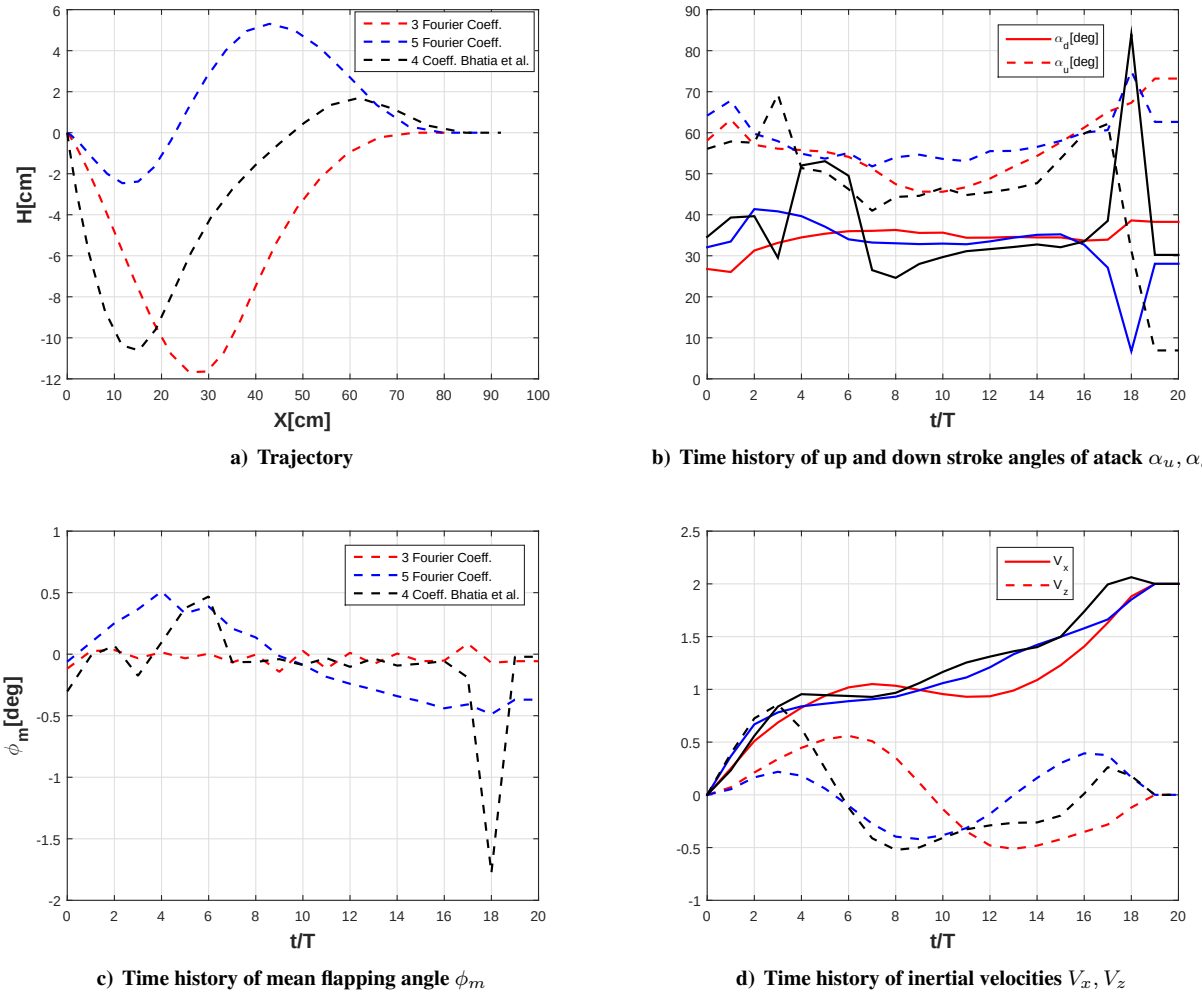


**a) Trajectory**

**b) Time history of up and down stroke angles of atack $\alpha_u, \alpha_d$**

**c) Time history of mean flapping angle $\phi_m$**

**d) Time history of inertial velocities $V_x, V_z$**

Figure 4

# References


[1] G. J. Berman and Z. J. Wang. Energy-minimizing kinematics in hovering insect flight. *Journal of Fluid Mechanics*, 582(1):153,168, 2007.

[2] M. Kurdi, B. Stanford, and P. Beran. Kinematic optimization of insect flight for minimum mechanical power. AIAA paper 2010-1420, Jan 2010.

[3] H. E. Taha, M. R. Hajj, and A. H. Nayfeh. Wing kinematics optimization for hovering micro air vehicles using calculus of variation. *Journal of Aircraft*, 50(2):610–614, 2013.

[4] B. K. Stanford and P. S. Beran. Analytical sensitivity analysis of an unsteady vortex-lattice method for flapping-wing optimization. *Journal of Aircraft*, 47(2):647–662, 2010.

[5] M. Ghommem, M. R. Hajj, B. K. Mook, D. T.and Stanford, R. D. Beran, P. S.and Snyder, and L. T. Watson. Global optimization of actively morphing flapping wings. *Journal of Fluids and Structures*, 33:210–228, 2012.

[6] L. Schenato, D. Campolo, and S. S. Sastry. Controllability issues in flapping flight for biomemetic mavs. volume 6, pages 6441–6447. 42nd IEEE conference on Decision and Control, 2003.

[7] D. B. Doman, M. W. Oppenheimer, and D. O. Sigthorsson. Wingbeat shape modulation for flapping-wing micro-air-vehicle control during hover. *Journal of Guidance, Control and Dynamics*, 33(3):724–739, 2010.

[8] M. W. Oppenheimer, D. B. Doman, and D. O. Sigthorsson. Dynamics and control of a biomimetic vehicle using biased wingbeat forcing functions. *Journal Guidance, Control and Dynamics*, 34(1):204–217, 2011.

[9] H. E. Taha, M. R. Hajj, and A. H. Nayfeh. Flight dynamics and control of flapping-wing mavs: A review. *Nonlinear Dynamics*, 70(2):907–939, 2012.

[10] H. E. Taha, M. R. Hajj, A. H. Roman, and A. H. Nayfeh. A calculus of variations approach for optimum maneuverability of flapping mavs near hover. *Journal of Guidance Control and Dynamics*, 37(4):167–1372, 2014.

[11] T. Weis-Fogh. Quick estimates of flight fitness in hovering animals, including novel mechanisms for lift production. *Journal of Experimental Biology*, 59(1):169–230, 1973.

[12] C. P. Ellington. The aerodynamics of hovering insect flight: III. kinematics. *Philosophical Transactions Royal Society London Series B*, 305:41–78, 1984.

[13] D. O. Sigthorsson, M. W. Oppenheimer, and D. B. Doman. Flapping wing micro-air-vehicle control employing triangular wave strokes and cycle-averaging. AIAA-paper 2010-7553, Aug 2010.

[14] R. J. Wood. The first takeoff of a biologically inspired at-scale robotic insect. *IEEE Transactions on Robotics and Automation*, 24(2):341–347, 2008.

[15] H. E. Taha, A. H. Nayfeh, and M. R. Hajj. Aerodynamic-dynamic interaction and longitudinal stability of hovering mavs/insects. Number AIAA-Paper 2013-1707, Apr 2013.

[16] Haithem E Taha, Muhammad R Hajj, and Ali H Nayfeh. Longitudinal flight dynamics of hovering mavs/insects. *Journal of Guidance, Control and Dynamics*, 2014. doi: 10.2514/1.62323.

[17] H. K. Khalil. Nonlinear systems. 2002. 3rd ed., Prentice–Hall, Upper Saddle River, NJ.

[18] J. Guckenheimer and P. Holmes. *Nonlinear Oscillations, Dynamical Systems, and Bifurcations of Vector Fields*. Academic Press, New York, NY, 1983.

[19] Haithem E Taha, Sevak Tahmasian, Craig A Woolsey, and Ali H Nayfehand Muhammad R Hajj. The need for higher-order averaging in the stability analysis of hovering, flapping-wing flight. *Bioinspir. Biomim.*, 2015.

[20] Manav Bhatia, Mayuresh Patil, Craig Woolsey, Bret Stanford, and Philip Beran. Stabilization of flapping-wing micro-air vehicles in gust environments. *Journal of Guidance, Control, and Dynamics*, 37(2):592–607, 2014.

[21] Michael W Oppenheimer, David B Doman, and David O Sigthorsson. Dynamics and control of a biomimetic vehicle using biased wingbeat forcing functions. *Journal of guidance, control, and dynamics*, 34(1):204–217, 2011.

[22] Alexander P Willmott and Charles P Ellington. The mechanics of flight in the hawkmoth manduca sexta. i. kinematics of hovering and forward flight. *The Journal of Experimental Biology*, 200(21):2705–2722, 1997.